Chapter 3

To investigate the therapeutic potential of small molecule enhancers for secretion of adiponectin (pitavastatin) and GLP-1 (L-glutamine)in T2D mouse model

3.1. Introduction

Insulin resistance, reduced insulin secretion, increased hepatic glucose output, dyslipidaemia/ hypercholesterolemia and β-cell degeneration lays the background for the onset of type 2 diabetes (T2D) (Pramanik *et al*., 2017). Many therapeutic modalities have been investigated to manage hyperglycaemia and the choice of drug varies from case to case. Though the initial borderline or pre-diabetic state management is relatively easy by combining lifestyle changes and dietary interventions, a progressed state of T2D needs to be addressed with respect to β-cell regeneration to boost insulin sensitivity. Most often at diagnosis, islet function might be reduced by 50% and β-cell mass by 60%. The reduction in β-cell mass is due to accelerated apoptosis (Garber, 2011). Autopsy studies conducted on T2D cadavers have shown 0-65% loss in β-cell mass (Matveyenko and Butler, 2008). Butler *et al*. showed that cadaver pancreatic autopsy of obese patients with pre-diabetes and T2D showed 40% reduction in β-cell mass as compared to obese individuals without T2D (Butler *et al*., 2003). Only a handful of current treatment modalities address the worsening condition of β-cell loss with time. We believe that the currently available on-shelf drugs have untapped potentials to reverse and restore glucose homeostasis. Enhancing the incretin glucagon-like peptide 1 (GLP-1) levels is one such intervention, which has a number of protective effects on β-cells, including a reduction in apoptosis and enhancement of β-cell proliferation and neogenesis (Garber, 2011). L-glutamine is known to stimulate secretion of GLP-1 in human subjects by raising cytosolic Ca^{2+} and cAMP in intestinal L-cells (Tolhurst *et al*., 2011). Interestingly, L-glutamine levels in prediabetics were reported to be higher (Owei *et al*., 2019), and they were found to be low in T2D subjects (Tsai *et al*., 2012; Chen *et al*., 2019). Another class of drugs, statins are known to induce new onset diabetes, but are used for the comprehensive management of hypercholesterolemia associated obesity induced T2D (Kim *et al*., 2019). Pitavastatin has shown a remarkable outcome on the glycemic control in T2D patients compared to other members of the statin group (Mita *et al*., 2013, Zhao and Zhao, 2015).

Thus, we hypothesize that the combination of two small-molecules, i.e., pitavastatin and L-glutamine can ameliorate high fat diet (HFD) and streptozotocin (STZ) induced T2D in C57BL6/J mice.

3.2. Materials and Methods

3.2.1 Animals and experimental strategy

9-10 weeks old (22 grams) male C57BL6/J mice procured from Advanced Centre for Treatment, Research and Education in Cancer (Navi-Mumbai, India) were housed in our animal house (Dept. of Biochemistry, The Maharaja Sayajirao University of Baroda, Vadodara, Gujarat, India), and maintained in a 12h:12h light-dark cycle, with free access to normal chow diet (NCD) /HFD (Keval Sales Corporation, India) and water *ad libitum*.

Based on the blood glucose levels and body weight, the animals were divided randomly first into two groups; NCD fed a normal chow diet (n=6) and another HFD (n=25) to develop obesity induced insulin resistance. After 20 weeks the HFD fed mice were administered three consecutive doses of streptozotocin (STZ) (MP Biomedicals, India) (40 mg/kg i.p.) to induce β-cell loss (Parilla *et al*., 2018). HFD+STZ induced T2D was confirmed with body weight (b.w.) ≥30 grams and three consecutive readings of fasting blood glucose (FBG) ≥240 mg/dL (Fig 3.1A).

After the 22nd week, HFD+STZ group was further divided randomly into four groups (n=6/group) i) HFD+STZ, ii) pitavastatin (P, 0.5mg/kg b.w. in diet) (Zambarakji *et al*., 2006), iii) L-glutamine (LG, 500mg/kg b.w. p.o.) (Badole *et al*., 2014; Sadar *et al*., 2016) and iv) pitavastatin (0.5mg/kg b.w. in diet) + L-glutamine (P+LG, 500mg/kg b.w. p.o.) treated (Fig 3.1B). The treatment was continued daily for six weeks along with 5-bromo-2'-deoxyuridine (BrdU) (MP Biomedicals, India) on alternate days (100mg/kg b.w. i.p.). FBG and BW of the animals were measured weekly using a glucometer (TRUEresult®- Nipro) and a weighing scale, respectively. Simultaneously, food and water intake were also measured. After six weeks of drug treatment, glucose tolerance and insulin tolerance were evaluated by intraperitoneal glucose tolerance test (IPGTT) and intraperitoneal insulin sensitivity test (IPIST). Mice were fasted for six hours and injected with glucose (2g/kg b.w.) and insulin (0.5U/kg) for IPGTT and IPIST (Jørgensen *et al*., 2017; Guo *et al*., 2018). 800-900µL blood was collected from orbital sinus and animals were euthanized for tissue collection. Plasma was separated and was stored for further biochemical analysis (Figure 3.1A).

All the procedures followed the institutional guidelines approved by Institutional Ethical Committee for Animal Research (IECHR), Faculty of Science, The Maharaja Sayajirao University of Baroda, Vadodara, Gujarat, India (MSU/BIOCHEMISTRY/IAEC/2018-21).

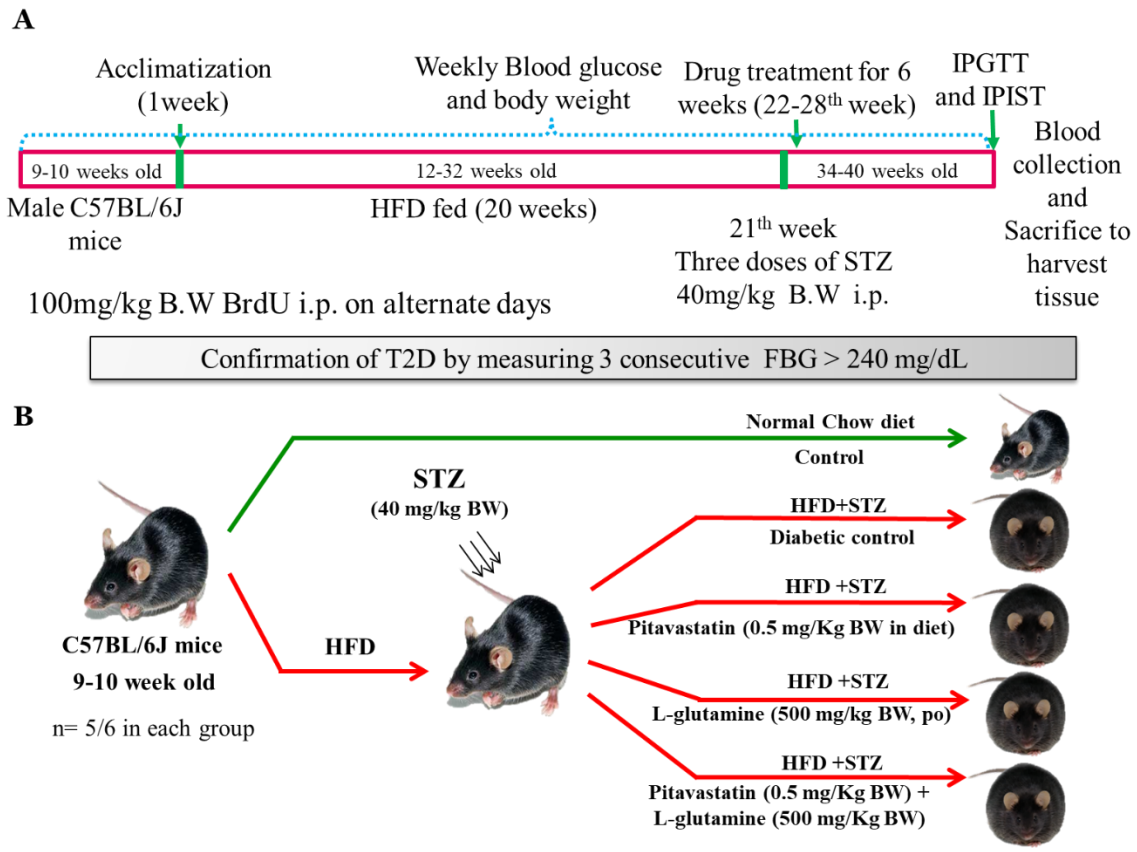

Figure 3.1 A) The experimental timeline: ~9-10 weeks old male C57BL/6J mice were subjected to 1 week acclimatization and weekly food intake, water consumption, BW and FBG levels were monitored throughout the study period. Post acclimatization they were divided into two groups: control group was fed with normal chow diet (NCD) and 20 weeks of HFD treatment was given to the second group to induce obesity and insulin resistance. On the 21st week, the HFD fed mice received three consecutive doses of STZ (40 mg/kg i.p.) to induce β-cell loss. T2D was confirmed with FBG measuring >240mg/dL. The T2D animals were further randomly divided into four groups for 6 weeks therapy. BrdU (100 mg/Kg b.w. i.p.) was administered on alternate days for the entire treatment period. The animals were then sacrificed and tissues were harvested for further analysis. **B) Strategy for drug treatment:** Animals were divided into two groups; one control group, fed with normal chow diet (NCD, n=6) and another T2D group (HFD+STZ, n=25) which was further divided into four groups (n=6/group): HFD+STZ (Diabetic control), pitavastatin (0.5mg/kg b.w. in diet), L-glutamine (500mg/kg b.w. p.o.) and pitavastatin (0.5mg/kg b.w. in diet) + L-glutamine (500mg/kg b.w. p.o.). The drugs were administered daily for 6 weeks.

3.2.2 Metabolic and Biochemical Parameters

3.2.2.1 Lipid profiling:

Plasma was used for lipid profiling (total cholesterol, triglycerides, high density lipoprotein) were measured by commercially available kits (Reckon Diagnostics Pvt. Ltd., Vadodara, GJ, India). Friedewald's (1972) formula was used for calculating low density lipoprotein (LDL) (Knopfholz *et al*., 2014).

3.2.2.2 Estimation of plasma insulin and adiponectin levels:

Insulin and adiponectin levels in plasma of the experimental animals were determined by mouse ELISA kits (RayBio, USA) as per manufacturers' instructions.

3.2.3 Assessment of transcript levels

Liver and skeletal muscle were collected and stored in RNAlater™ Stabilization Solution (Thermo Fisher Scientific, USA) and total RNA was extracted by the Trizol method. RNA integrity and purity were verified by 1.5% agarose gel electrophoresis/ethidium bromide staining and O.D. 260/280 absorbance ratio of 1.9 respectively. To avoid DNA contamination, RNA was treated with DNase I (Puregene, Genetix Biotech) before cDNA synthesis. Transcriptor High Fidelity cDNA Synthesis Kit (Roche Diagnostic GmbH, Mannheim, Germany) was used to prepare cDNA using one microgram of total RNA isolated, according to the manufacturer's instructions in the Eppendorf Mastercycler gradient (USA Scientific, Inc., Florida, USA). The expression of enlisted gene transcripts was measured by Light-Cycler® 480 Real-time PCR (Roche Diagnostics GmbH, Manneheim, Germany) using gene- specific primers (Eurofins, Bangalore, India) as shown in Table 3.1. Real-time PCR was performed using Light-CyclerH 480 SYBR Green I Master (Roche Diagnostics GmbH, Mannheim, Germany) and carried out in the Light-CyclerH 480 Real-Time PCR (Roche Diagnostics GmbH, Mannheim, Germany).

Table 3.1: Primers for the transcript analysis

Gene/ Primer	Sequence	Annealing temperature	Amplicon size	Tissue
Glucokinase (GCK)				Liver
FP	5'-AGGAGGCCAGTGTAAAGATGT-3'	56°C	90 bps	

RP	5'-TCCCAGGTCTAAGGAGAGAAA-3'			
Phosphoenolpyruvate carboxykinase (PEPCK)				
FP	5'-CTGCATAACGGTCTGGACTTC-3'	65°C	151 bps	
RP	5'-CAGCAACTGCCCGTACTCC-3'			
Glucose 6 phosphatase (G6Pase)				
FP	5'-CTGTTTGGACAACGCCCGTAT-3'	56°C	91 bps	
RP	5'-AGGTGACAGGGAACTGCTTTA-3'			
Glucose transporter 2 (GLUT2)				
FP	5'-CTTGGAAGGATCAAAGCAATG-3'	60°C	150 bps	
RP	5'-CAGTCCTGAAATTAGCCCAC-3'			
Glycogen Synthase				
FP	5'-ACCAAGGCCAAAACGACAG-3'	61°C	102 bps	
RP	5'-GGGCTCACATTGTTCTACTTG-3'			
Fructose 1,6, bisphosphatase (FBPase)				
FP	5'-GCATCGCACAGCTCTATGGT-3'	63°C	120 bps	
RP	5'-CTCAGGTTCGATTATGATGGC-3'			
Glycogen Phosphorylase				
FP	5'-GAGAAGCGACGGCAGATCA-3'	65°C	102 bps	
RP	5'-CTTGACCAGAGTGAAGTGCA-3'			
Sirtuin 1 (SIRT1)				
FP	5'-GATGAAGTTGACCTCCTCA-3'	64°C	86 bps	
RP	5'-GGGTATAGAACTTGGAATTAG-3'			
Peroxisome proliferator-activated receptor-gamma coactivator (PGC1α)				Skeletal Muscle
FP	5'-AGCCGTGACCACTGACAACGA-3'	69°C	129 bps	
RP	5'-GTAGCTGAGCTGAGTGTTGGC-3'			
Transcription factor A (TFAM)				
FP	5'-CTGAGGAAAAGCAGGCATA-3'	69°C	142 bps	
RP	5'-ATGTCTCCGGATCGTTTCAC-3'			
Glyceraldehyde 3-phosphate dehydrogenase (GAPDH)				Liver, Skeletal Muscle
FP	5'-AGGTCGGTGTGAACGGATTTG-3'	56°C	123 bps	
RP	5'-TGTAGACCATGTAGTTGAGGT-3'			

FP: Forward Primer; RP: Reverse Primer; bp: base pair

3.2.4 Glucoregulatory enzymes activities and liver glycogen content:

Liver was harvested, snap freezed using dry ice and stored at -80°C. 50 mg of liver tissue was homogenized and tissue lysates were used for the activity assays. Enzyme assays for glucokinase (GCK), Fructose 1,6-bisphosphatase (FBPase), Phosphoenolpyruvate carboxykinase (PEPCK), and glycogen content were carried out using commercially available kits (BioVision, Milpitas, CA, USA) according to the manufacturers' protocols.

3.2.5 Mitochondrial isolation from skeletal muscle and estimation of oxygen consumption rate (OCR)

For OCR studies, skeletal muscle from hind leg was harvested post euthanization and stored in mitochondrial respiration buffer at -80 °C. Mitochondria were isolated from 120mg skeletal muscle using mitochondria isolation kit (Thermo Scientific^{TM}, Catalog no. 89801) using manufacturer's protocol. The isolated mitochondria were resuspended in mitochondria respiration buffer (110mM sucrose, 0.5mM EGTA, 70 mM KCl, 0.1% FFA free BSA, 20 mM HEPES, 3 mM $MgCl_2$, and 10 mM KH_2PO_4, 20mM taurine) (Butterick *et al*, 2016). Mitochondrial outer membrane integrity of the isolated mitochondria was assessed by impermeability to exogenous cytochrome c which was consistently greater than 95%. Respiratory chain complexes I-III activities were recorded using 100 mM pyruvate & 800 mM malate (complex I), 1M succinate (complex II) and 10 mM α-glycerophosphate (complex III) as the respective substrates (Li and Graham, 2012) added to 90 µl of mitochondria suspension in respiration buffer. Other respiration reagents used were 100 mM adenosine diphosphate (100 µl), 1 mM oligomycin (2 µl), 1 mM rotenone (1 µl), and 1 mM antimycin (2.5 µl). All chemicals were purchased from Sigma-Aldrich, USA. Protein concentration was estimated by Bradford method (Stoscheck *et al*., 1990). OCR was determined by measuring the amount of oxygen (nmol) consumed, divided by the time elapsed (min) and the amount of protein present in the assay (Li and Graham, 2012).

3.2.6 Pancreatic tissue preparation, Immunohistochemistry-Immunofluorescence (IHC-IF), assessment of β-cell regeneration and apoptosis

Pancreas was harvested and fixed in 10% neutral buffered formalin (NBF) for paraffin embedding. 5µm sections of the paraffin embedded blocks were made. Immunofluorescence staining was carried out to detect β-cell regeneration by proliferation (insulin/Glucagon/BrdU), neogenesis (insulin/Nng3/Pdx1), and α- to β-cell transdifferentiation (insulin/Arx/Pax4). β-cell apoptosis was detected by terminal deoxynucleotidyl transferase dUTP nick end labelling (TUNEL) assay (insulin/ fluorochrome tagged deoxynucleotides) (Thermo Fisher Scientific, MA, USA) and apoptosis inducing factor (AIF) translocation into the nucleus (insulin/AIF). The sections were deparaffinized in xylene and rehydrated in a series of diluted ethanol (100%, 95%, 80% and 70%). Slides were then treated with 1N HCl for 40 minutes at 37°C for antigen retrieval followed by blocking in 5% donkey serum diluted in PBST (PBS + 0.1% tween 20) for 1 hour at room temperature. The slides were then incubated with the respective primary antibodies prepared in blocking buffer at 37°C in a humidified chamber for 2 hours [guinea pig anti-insulin, rabbit anti-glucagon, rat anti-BrdU, rabbit anti-Ngn3, goat anti-Pdx1, rabbit anti-Arx, goat anti-Pax4, and rabbit anti-AIF]. Sections were washed with PBS and were incubated with secondary antibodies prepared in blocking buffer at room temperature for 45 minutes in dark [donkey anti-guinea pig Alexa Fluor 488, donkey anti-rabbit Alexa Fluor 647, donkey anti-goat Rhodamine Red X, donkey anti-rat Rhodamine Red X, donkey anti-guinea pig Alexa Fluor 568 (Table 3.2)]. Pancreatic sections were washed with PBS and distilled water and were mounted with Slowfade^{TM} Gold Antifade mountant with DAPI (Thermo Fisher Scientific, USA), and coverslips were sealed with nail varnish. Stained sections were observed under confocal laser scanning microscope (Olympus FV10i, Tokyo, Japan). Image analysis was carried out in Image J software. Observations were made from three pancreatic sections per group from five different areas.

Table 3.2: Details of the antibodies used for IHC-IF.

Primary Antibody	**Secondary Antibody**	**Excitation (nm)**	**Emission (nm)**
Anti-insulin (1:100, guinea pig) [DAKO Agilent, USA]	Alexa 488 (1:500, Donkey) [Jackson ImmunoResearch Laboratories, Inc. USA]	493	519
Anti-Ngn3 (1:50, rabbit)	Alexa 647 (1:500, Donkey)	651	667

[Thermo Fisher Scientific, USA]	[Jackson ImmunoResearch Laboratories, Inc. USA]		
Anti-Arx1 (1:500, Rabbit) [Sigma-Aldrich, Germany]			
AIF (1:400)			
Anti-glucagon (1:200, rabbit) [Cell Signaling Technology, USA]			
Anti-Pdx1 (1:1000, Goat) [Abcam, USA]	Rhodamine Red (1:200, Donkey) [Jackson ImmunoResearch Laboratories, Inc. USA]	570	590
Anti-Pax4 (1:500, Goat) [Sigma-Aldrich, Germany]			
Anti-BrdU (1:100, Goat) [Abcam, USA]	Rhodamine Red (1:200, Rat) [Jackson ImmunoResearch Laboratories, Inc. USA]	570	590

3.2.7 Western blot analysis:

Skeletal muscle was harvested and freezed in dry ice and stored at -80 °C for western blot analysis of key proteins involved in insulin signalling pathway. The tissue was homogenized in liquid nitrogen and Laemmli buffer (1M Tris HCl, 10% SDS, 20% glycerol and 10% β-mercaptoethanol) containing 1M urea (1:1), protease inhibitor cocktail, and phosphatase inhibitor cocktail 2 and 3 (Sigma, St. Louis, MO, USA). The homogenate was further sonicated twice in chilled condition and centrifuged to remove tissue/cell debris. Protein concentration in the lysates were estimated using Bradford method after TCA precipitation and 25-40 µg of protein was resolved on 8-10% SDS-PAGE, followed by electrophoretic transfer to PVDF membrane. The membrane was blocked with 5% bovine serum albumin (BSA) (Hi-Media, India) prepared in tris-buffered saline (pH 8.0) with 0.1% tween-20 for one hour at room temperature followed by overnight incubation in the respective primary antibodies. The membrane was incubated with the respective secondary antibodies conjugated with HRP (Table 3.3) at room temperature for 1 hour. Four washes of 1% PBST was given before and after secondary antibody incubation. The membrane was visualized with the clarity western ECL substrate (Bio-Rad Laboratories, USA) in ChemiDoc™ Touch

Imaging System and blots were analysed in Image lab™ software (Bio-Rad Laboratories, USA).

Table 3.3: Details of the antibodies used for western blot

Primary antibody	**Secondary antibody**
Anti-β-actin (1:10,000, mouse) [ABclonal Technology, USA]	Anti-mouse IgG-HRP (1: 10,000, goat) [Santa Cruz Biotechnology]
Anti-insulin receptor β (1:1000, rabbit) [Cell Signaling Technology, USA]	Anti-rabbit immunoglobulin G (IgG)-horse radish peroxidase (HRP) (1:5000, goat) [Santa Cruz Biotechnology]
Anti-insulin receptor substrate-1 (1:1000, rabbit) [ABclonal Technology, USA]	
Anti-phosphorylated insulin receptor substrate -1 Ser307 (1:1000, rabbit) [Cell Signaling Technology, USA]	
Anti- Akt-1 (Protein kinase B) (1:1000, rabbit) [ABclonal Technology, USA]	
Anti-phosphorylated Akt-1(Protein kinase B) S473 (1:1000, rabbit) [ABclonal Technology, USA]	
Anti-Glut 4 (Glucose transporter type 4) (1:1000, rabbit) [MERCK Millipore]	
Anti-AdipoR1 (Adiponectin receptor 1) (1:1000, rabbit) [Bioss Antibodies, USA]	
Anti-PPARa (Peroxisome proliferator activated receptor alpha) (1:1000, rabbit) [Bioss Antibodies, USA]	

3.2.8 Statistical analyses:

The data analysed are expressed as the mean ± SEM and $p<0.05$ was considered as significant. The difference between groups was calculated by one-way ANOVA followed by the Tukey's test for multiple group analysis. All the analyses were carried out in GraphPad Prism 5 software.

3.3. Results

3.3.1 Animals and experimental strategy to develop T2D mouse model:

After 20 weeks of HFD treatment, animals became obese and insulin resistant. After STZ administration, the FBG levels of these animals surpassed 240 mg/dl (Figure 3.2 A). There was significant increase in the FBG levels and BW post STZ treatment (Figure 3.2 B & C).

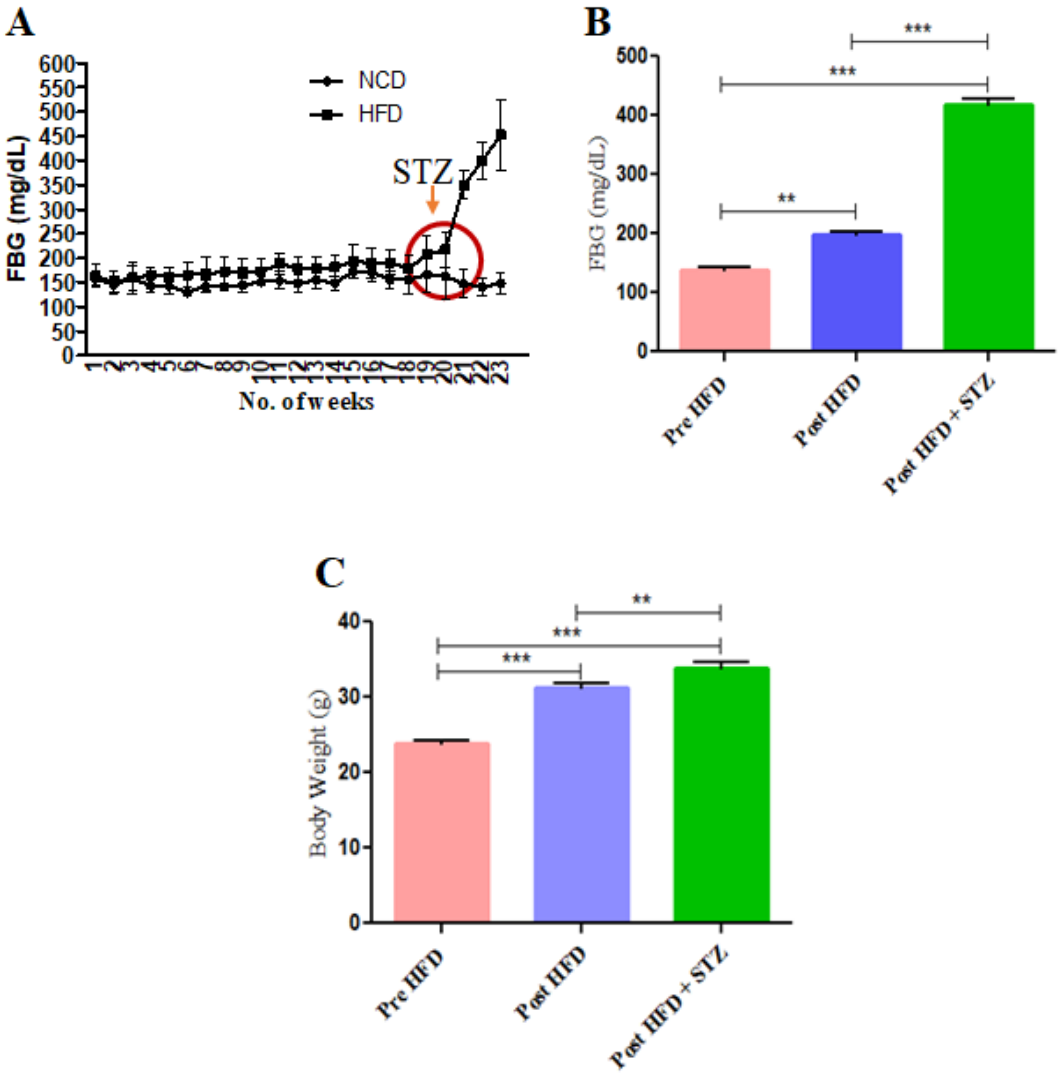

Figure 3.2. A) Fasting blood glucose (FBG) levels in insulin resistance mouse model. STZ administered at the 20th week showed FBG> 240 mg/dL. **B) FBG levels in experimental diabetic mice (pre- and post- HFD, and HFD+STZ treated mice).** A significant difference in FBG levels was observed in the animals before and after HFD, and

HFD+STZ treatment as compared to NCD mice (**p<0.01, ***p<0.001 respectively). **C) Body weight of experimental diabetic mice (pre- and post- HFD, and HFD+STZ treated).** A significant difference in the body weight was observed in the HFD and HFD+STZ mice as compared to NCD mice (***p<0.001, ***p<0.001 respectively).

3.3.2 Assessment of metabolic and biochemical parameters:

There was significant rise in the FBG levels and body weight in HFD+STZ group (p<0.001 and p<0.01) as compared to NCD. At the end of six weeks of drug treatment significant reduction in FBG levels of P (p<0.05), LG (p<0.05) and P+LG (p<0.001) groups, (Fig. 3.3 A) and significant decrease in the body weight of P (p<0.001), LG (p<0.05) and P+LG (p<0.01) groups as compared to HFD+STZ group (Fig. 3.3 B) were observed.

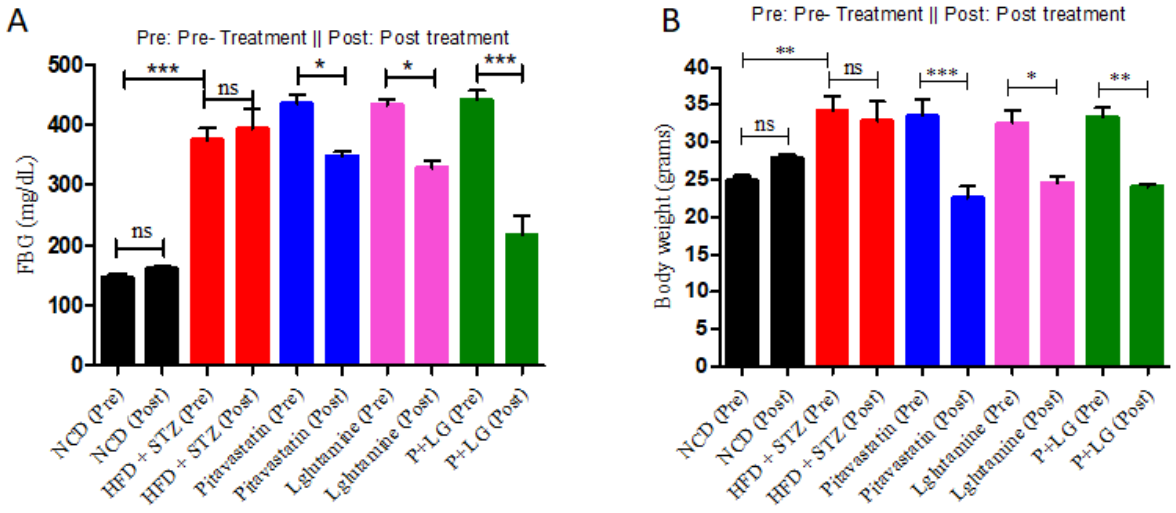

Figure 3.3. Fasting blood glucose (FBG) and body weight (BW) in drug treated groups: A) Significant increase in FBG levels was seen in HFD+STZ group. A significant decrease in the FBG levels was observed in monotherapy treated groups which was further reduced in combination (P+LG) treated group as compared to pre-treatment, **B)** Significant increase in body weight was seen in HFD+STZ group. A significant decrease in body weight was observed in monotherapy treated and combination treated groups as compared to pre-treatment (ns=non-significant, *p<0.05, **p<0.01, ***p=0.001, Pre vs. Post; n=5/group).

3.3.2.1 Intraperitoneal glucose tolerance test (IPGTT) and Intraperitoneal insulin sensitivity test (IPIST):

HFD+STZ group showed a sharp rise in FBG levels post glucose administration which took longer time to resolve back to its basal level. Monotherapy treated groups showed higher base line glucose after four hours fasting. However, in spite of a sharp rise in the glucose levels of monotherapy groups the drop at 30 minutes and thereafter, was faster indicating their improved glucose tolerance as compared to HFD+STZ group. The basal FBG levels in mice treated with P+LG were significantly lower and coincided with NCD as compared to HFD+STZ group (Figure 3.4 A). Area under the curve (AUC) 0–120 curve indicated improved glucose tolerance in the P+LG group as compared to HFD+STZ group (Figure 3.4 B). FBG levels in P+LG group were significantly lower as compared to P and LG groups after 60, 90 and 120 minutes of insulin administration (Figure 3.4 C). AUC 0–120 curve in P+LG group was significantly lower as compared to HFD+STZ group after 60, 90 and 120 minutes of insulin administration (Figure 3.4 D).

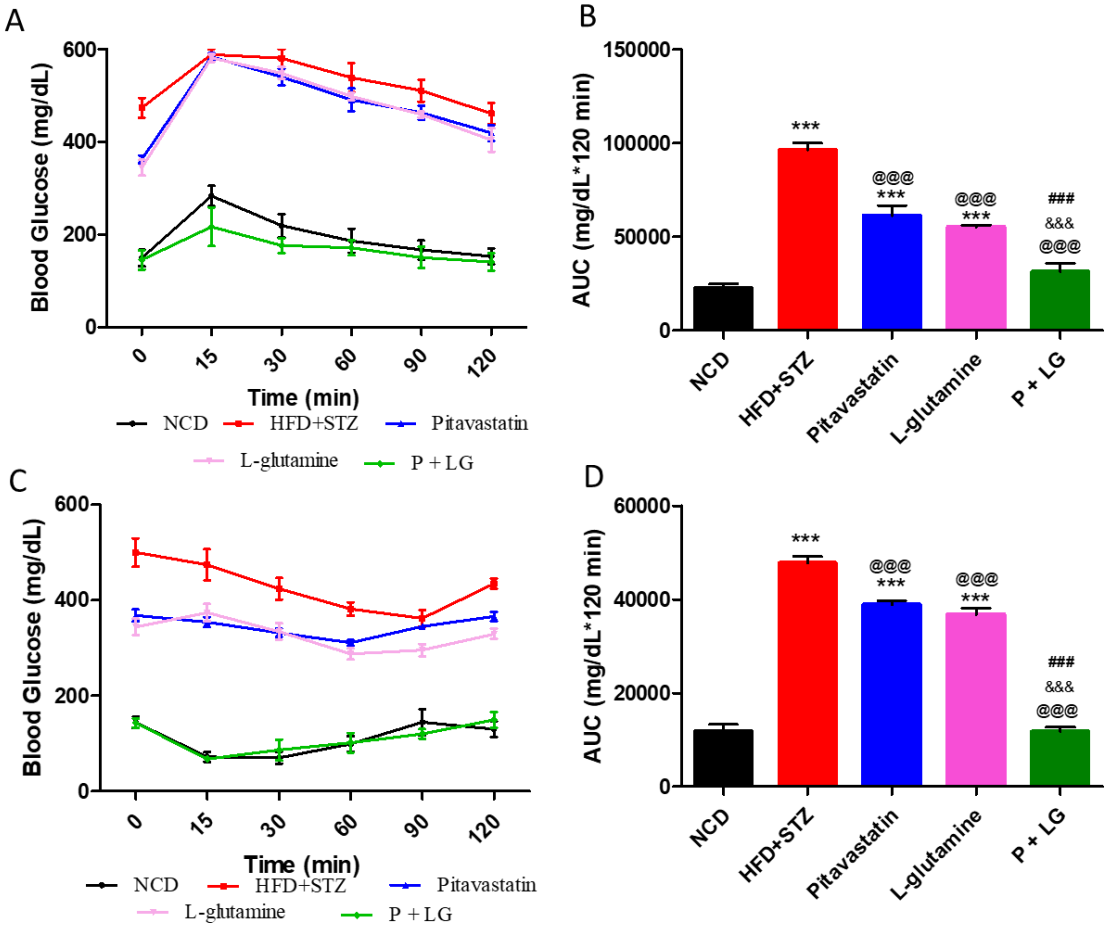

Figure 3.4. Intraperitoneal glucose tolerance test (IPGTT) (A-B) & intraperitoneal insulin sensitivity test (IPIST) (C-D) in the drug treated animals. A-B) Increased glucose

clearance was observed in the monotherapies as suggested by the AUC plot. The effect of P+LG on glucose AUC was significantly enhanced indicating improved glucose tolerance. Also, the glucose levels at the fasting time point (0) in the P+LG group was comparable with NCD; **C-D)** Insulin sensitivity was significantly increased in the monotherapies however the accentuated drop in the AUC of P+LG along with FBG levels at fasting time point (0) demonstrates the enhanced insulin sensitivity. **(**$^{@@@}p<0.001$ vs. HFD+STZ, $^{\&\&\&}p<0.001$ vs. P, $^{\#\#\#}p<0.001$ vs. LG, $^{***}p<0.001$ vs. NCD, n=5/ group).

3.3.2.2 Lipid profiling:

Triglycerides (TG), total cholesterol (TC), low density lipoprotein (LDL) and high-density lipoprotein (HDL) levels were significantly increased in the HFD+STZ group ($p<0.001$, $p<0.001$, $p<0.001$ and $p<0.05$, respectively) as compared to NCD. The increased HDL is indicative of increased reverse cholesterol transport through the HDL pathway, as an adaptation to the metabolic load of a high fat diet (Hayek *et al*., 1993). Upon six weeks of drug treatment the TG, TC and LDL levels were significantly reduced in the P+LG group ($p<0.001$, $p<0.001$ and $p<0.001$, respectively) as compared to HFD+STZ (Fig. 3.5 A, B & C). Further, HDL levels were significantly increased in the P and LG groups but were significantly decreased ($p<0.001$) in the P+LG group as compared to HFD+STZ and were at par with the HDL levels in NCD (Fig. 3.5 D).

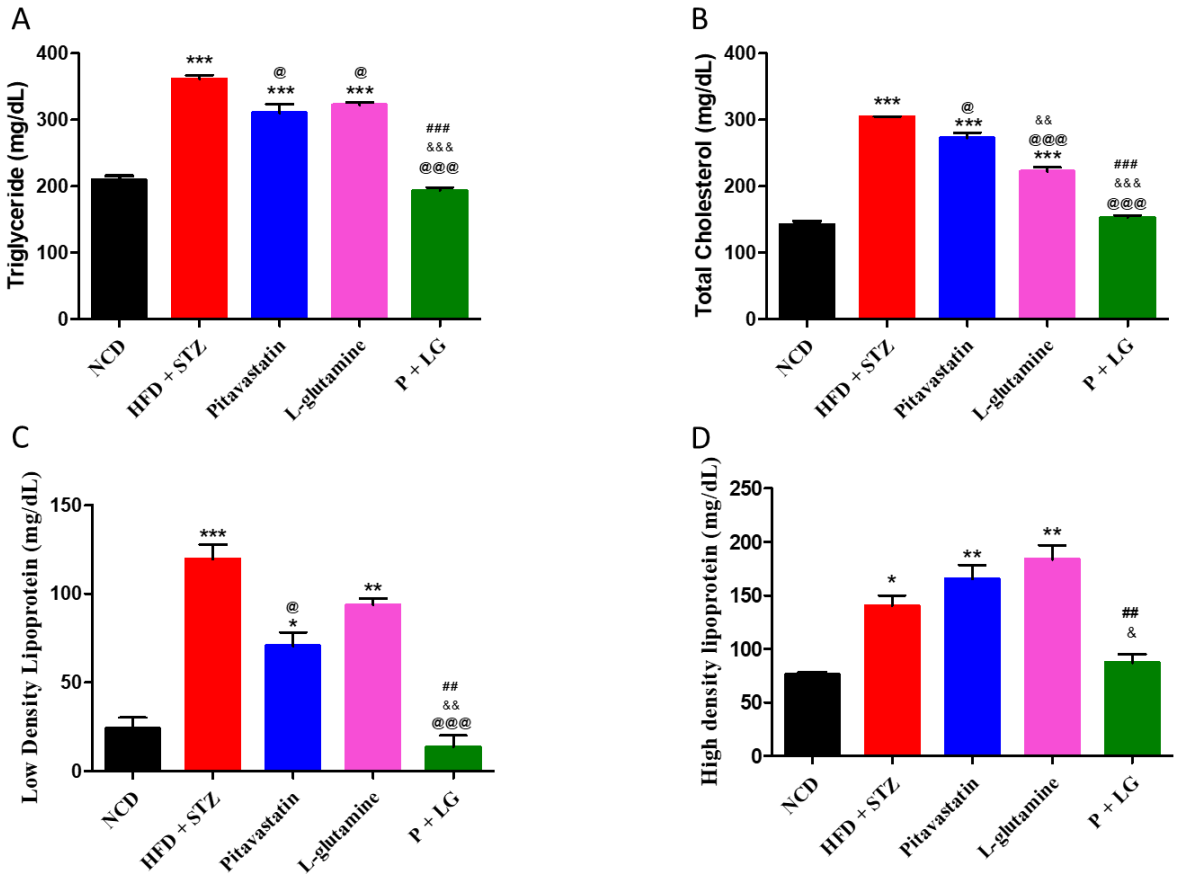

Figure 3.5. Plasma lipid profile: A) TG levels were significantly increased in HFD+STZ group and were significantly reduced in P, LG and P+LG groups. **B)** Total cholesterol levels were significantly increased in HFD+STZ group and were significantly reduced in P, LG and P+LG groups. **C)** LDL levels were significantly increased in HFD+STZ group and were significantly reduced only in P and P+LG groups as compared to HFD+STZ group. **D)** HDL levels were significantly increased in HFD+STZ, P and LG groups, and were significantly reduced in the P+LG group compared to HFD+STZ group ($^{@}p<0.05$, $^{@@@}p<0.001$ vs. HFD+STZ, $^{\&}p<0.05$, $^{\&\&}p<0.01$, $^{\&\&\&}p<0.001$, vs. P, $^{\#\#}p<0.01$, $^{\#\#\#}p<0.001$, vs. LG, $^{*}p<0.05$, $^{**}p<0.01$, $^{***}p<0.001$, vs. NCD, n=5/group).

3.3.2.3 Plasma insulin and adiponectin levels:

Significant decrease in insulin and adiponectin levels was observed in HFD+STZ group ($p<0.001$ and $p<0.05$) as compared to NCD. Upon six weeks of drug treatment significant increase in the insulin levels was observed in P ($p<0.05$), LG ($p<0.05$) and P+LG ($p<0.01$) groups (Fig 3.6 A). Further, the adiponectin levels were significantly increased in P

(p<0.001) and LG (p<0.05) groups while a normo-adiponectinemia was seen in the P+LG group (Fig 3.6 B).

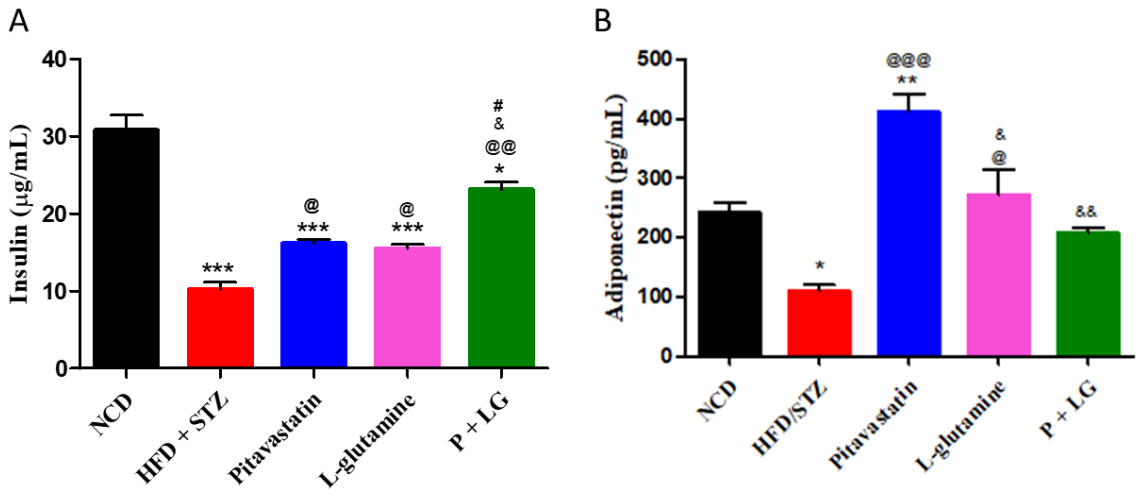

Figure 3.6. Plasma insulin & adiponectin levels: A) Significant decrease in insulin levels were observed in HFD+STZ group. Significant increase in insulin levels were observed in monotherapies which was further accentuated in the P+LG group. **B)** The HFD+STZ group showed significant decrease in adiponectin levels. Significant increase in adiponectin levels was observed in monotherapy groups as compared to HFD+STZ group and normo-adiponectinemia was observed in the combination group ($^{@}p$<0.05, $^{@@}p$<0.01, $^{@@@}p$<0.001, vs. HFD+STZ, $^{\&}p$<0.05, $^{\&\&}p$<0.01, vs. P, $^{\#}p$<0.05, vs. LG, *p<0.05, **p<0.01, ***p<0.001, vs. NCD, n=5/ group).

3.3.3 Gene expression of *GLUT2* and glucoregulatory enzymes and their activities in liver:

The gene expression, and activity of key enzymes involved in the glucoregulatory metabolic pathways were assessed in liver. HFD+STZ group showed significant decrease in *GCK* (glycolysis) expression (p<0.001) and activity (p<0.01) as compared to NCD (Figure 3.7 A & B). There was also significant increase in the FBPase and PEPCK (gluconeogenesis) expression (p<0.05, p<0.01) and activity (p<0.01, p<0.001) (Figure 3.7 C, D, E & F). In addition, the *G6pase* (gluconeogenesis) expression was increased in HFD+STZ group (p<0.01) while reduced *glycogen synthase* expression (p<0.05), glycogen content (p<0.01), and increased g*lycogen phosphorylase* (glycogenolysis) and *GLUT2* expression (p<0.05 and p<0.001) were observed in HFD+STZ group.

The P+LG group showed a significant increase in the *GCK* expression (p<0.01) and activity (p<0.01) (Figure 3.7 A & B) and increased expression of g*lycogen synthase* (glycogenesis) (p<0.01; Figure 3.7 H), and increased glycogen content (p<0.001; Figure 3.7 I). Further, a significant decrease in the expression and activity of FBPase and PEPCK (p<0.05, p<0.001 and p<0.001, p<0.001 respectively; Figure 3.7 C, D, E & F) along with a concomitant decrease in *G6Pase* expression (p<0.01; Figure 3.7 G) were observed in P+LG group. Additionally, the g*lycogen phosphorylase* expression was also reduced (p<0.001; Figure 3.7 J) in the combination-treated group with a concomitant decrease in *GLUT2* receptor expression (p<0.001; Figure 3.7 K).

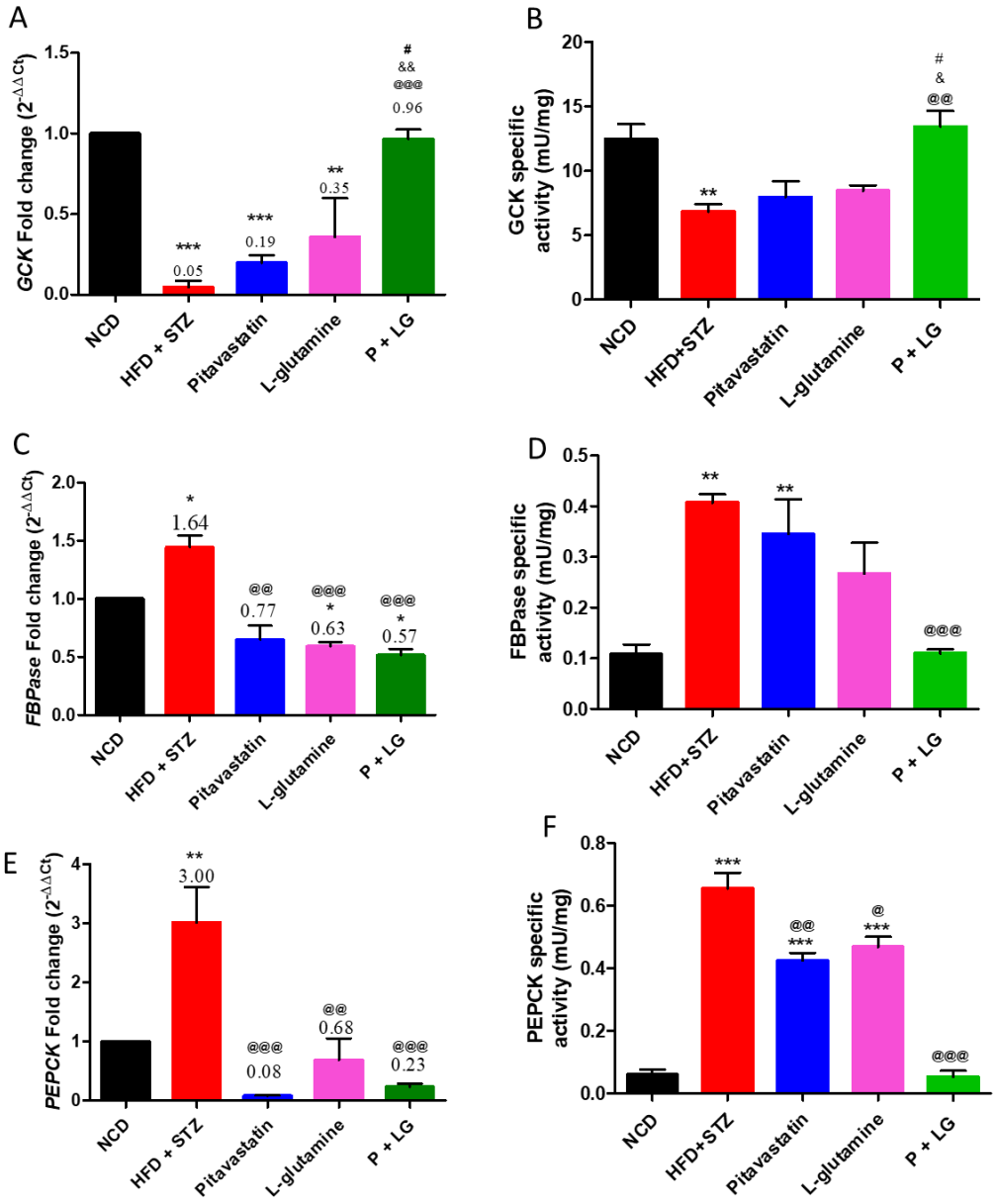

Figure 3.7. Glucoregulatory enzymes gene expression and activities in liver: A) *GCK* (glycolysis) expression: There was a 0.05-fold decrease in the *GCK* expression of HFD+STZ group as compared to NCD which was significantly increased in the P+LG treated group, **B)**

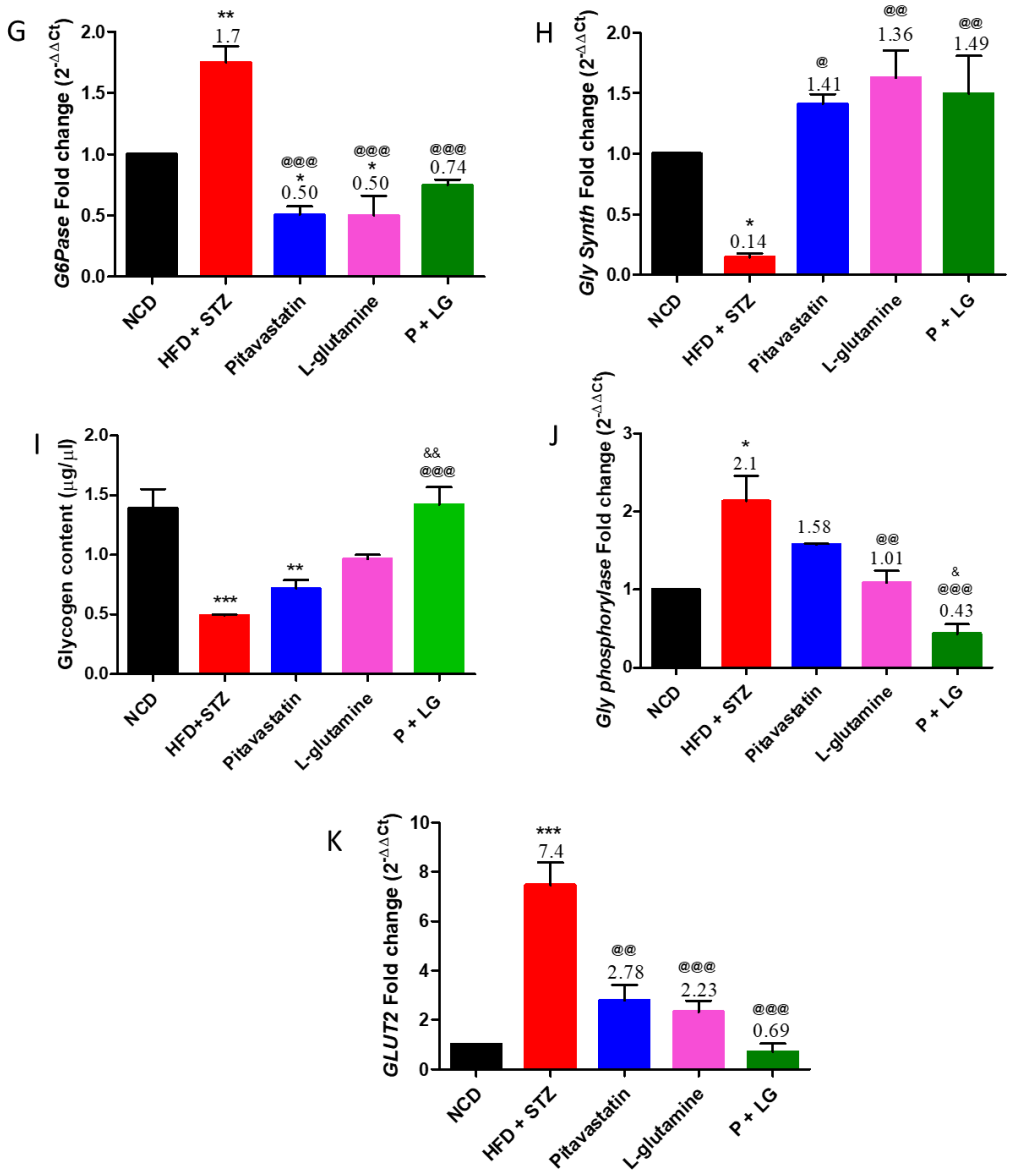

GCK activity: There was a significant decrease in the activity of GCK in the HFD+STZ group. Upon P+LG treatment there was a significant increase in the activity of GCK; **C) *FBPase* (gluconeogenesis) expression:** There was a 1.64-fold rise in the *FBPase* expression of HFD+STZ group as compared to NCD. The expression was significantly reduced in P (0.77-fold), LG (0.63-fold) and the P+LG (0.57-fold) groups, **D) FBPase activity:** There was a significant rise in the FBPase activity of HFD+STZ group as compared to NCD. The

enzyme activity levels were significantly reduced in the P+LG group as compared to HFD+STZ. **E) *PEPCK* (gluconeogenesis) expression:** There was a 3-fold rise in the *PEPCK* expression of HFD+STZ group as compared to NCD. A significant decrease in the expression of *PEPCK* was observed in P, LG and P+LG treated groups as compared to HFD+STZ, **F) PEPCK enzyme activity**: There was a significant rise in the PEPCK activity of HFD+STZ group as compared to NCD which was reversed upon combination treatment; **G) *G6Pase* (glucose 6 phosphatase) expression:** There was a significant increase in the *G6Pase* expression in HFD+STZ group as compared to NCD and was significantly reduced upon mono-and P+LG treated groups as compared to HFD+STZ. **H) *Glycogen Synthase* (Glycogenesis) expression:** There was a significant decrease in the expression of *Glycogen Synthase* in the HFD +STZ group as compared to NCD and a significant rise in the *Glycogen Synthase* expression in mono- and P+LG treated group as compared to HFD+STZ; **I) Glycogen content:** The glycogen content was significantly reduced in HFD+STZ group as compared to NCD. There was a significant increase in the glycogen content in the P+LG treated group as compared to HFD+STZ group; **J) *Glycogen phosphorylase* (glycogenolysis) expression:** There was a significant increase in the *Glycogen phosphorylase* expression in HFD+STZ group as compared to NCD. The *Glycogen phosphorylase* expression was significantly decrease in the P and P+LG treated groups as compared to HFD+STZ; **K) *GLUT2* gene expression:** There was a significant rise in the *GLUT2* expression of HFD+STZ group as compared to NCD. There was a significant decrease in the *GLUT 2* expression in P, LG and P+LG treated groups as compared to HFD+STZ. ($^{@}p$<0.05, $^{@@}p$<0.01, $^{@@@}p$<0.001, vs. HFD+STZ, $^{\&\&}p$<0.01, $^{\&\&\&}p$<0.001, vs. P, $^{\#}p$<0.05, vs. LG, **p*<0.05, ***p*<0.01, ****p*<0.001, vs. NCD, n=4-5/group)

3.3.4. Mitochondrial biogenesis markers' transcript levels in skeletal muscle:

A significant decrease in the expression of *SIRT1*, *PGC1α* and *TFAM* was observed in HFD+STZ group as compared to NCD (*p*<0.001, *p*<0.001 and *p*<0.05, respectively; Figure 3.8 A, B & C). A significant increase in the expression of *SIRT1* was observed in the monotherapies (*p*<0.05 and *p*<0.01) and P+LG (*p*<0.001) treated groups (Figure 3.8 A) along with a significant increase in the expression of *PGC1α* and *TFAM* in the monotherapies (*p*<0.05, *p*<0.05 and *p*<0.01, *p*<0.05, respectively) and P+LG (*p*<0.01 and *p*<0.001, respectively) treated groups (Fig 3.8 B & C).

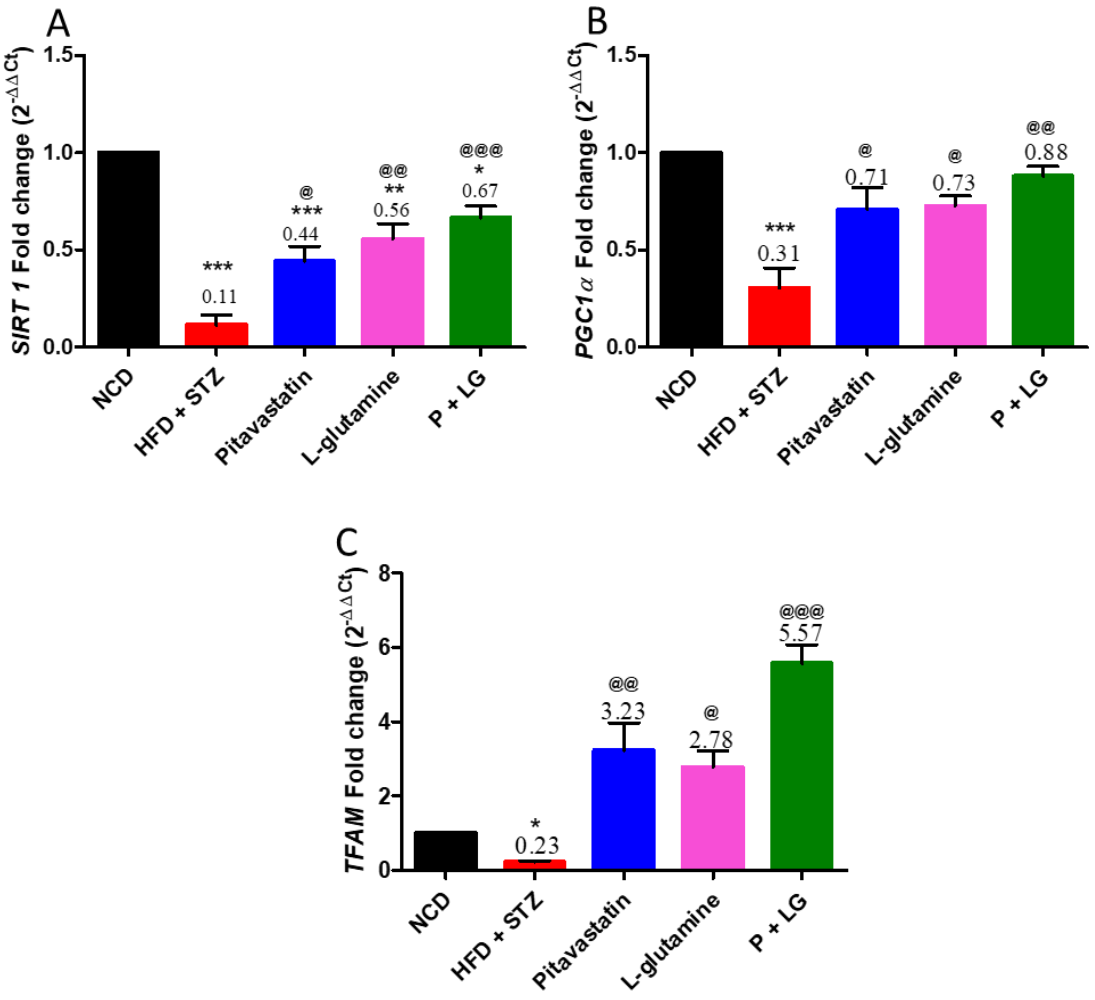

Figure 3.8. Mitochondrial biogenesis marker levels in skeletal muscle: A) *SIRT1:* There was a 0.11-fold decrease in the *SIRT1* expression in HFD+STZ group. A 0.44, 0.56 and 0.67-fold increase in the *SIRT1* expression were observed in the P, LG and P+LG treated groups respectively; **B) *PGC1α:*** There was a 0.31-fold decrease in the HFD+STZ group and the expression of *PGC1 α* in P, LG and P+LG treated groups showed 0.71, 0.73 and 0.88-fold increase in the *SIRT1* expression respectively, and **C) *TFAM*:** There was a 0.23-fold drop in the *TFAM* expression in HFD+STZ group which increased by 3.23, 2.78 and 5.57-fold in the P, LG and P+LG treated groups respectively ($^{@}p<0.05$, $^{@@}p<0.01$, $^{@@@}p<0.001$, vs. HFD+STZ, $*p<0.05$, $**p<0.01$, $***p<0.001$, vs. NCD, n=5/group).

3.3.5. Estimation of oxygen consumption rate (OCR)

The OCR of state 3/state 4 in HFD+STZ group was significantly reduced as compared to NCD for the mitochondrial complexes I, II and III ($p<0.001$, $p<0.01$ and $p<0.001$,

respectively; Figure 3.9 A, B & C). A significant increase in the OCR of P, LG and P+LG groups were observed in CI (p<0.01, p<0.05 & p<0.001; Figure 3.9 A) and CII (p<0.05, p<0.05 & p<0.001; Figure 3.9 B), respectively. However, the OCR of state 3/state 4 in complex III was significantly improved only in the P+LG treated group (p<0.001, p<0.001 and p<0.001, respectively; Figure 3.9 C) as compared to HFD+STZ.

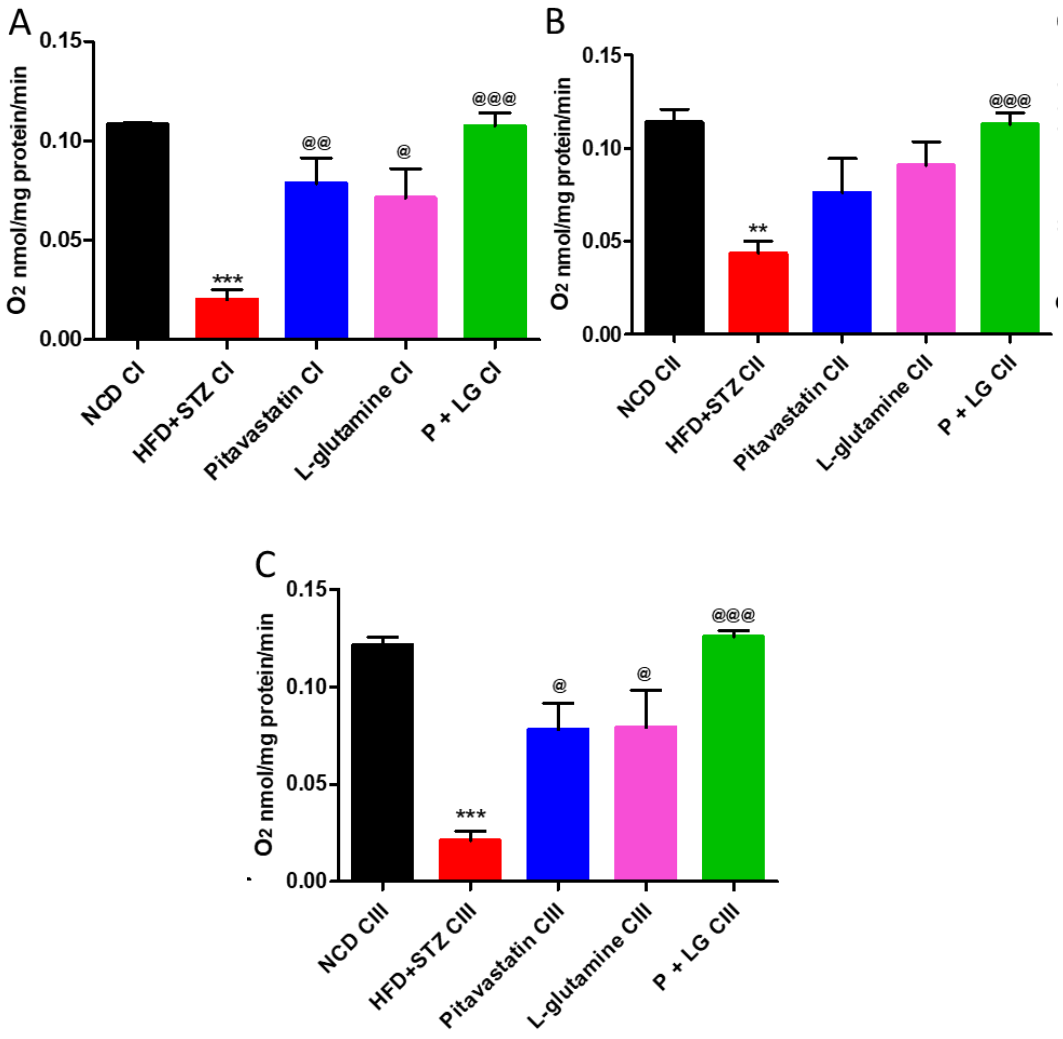

Figure 3.9: Ratio of oxygen consumption rate: A) Complex I: OCR of state 3/state 4 in HFD+STZ group was reduced as compared to NCD. There is a rise in the OCR in the P+LG treated group; **B) Complex II:** OCR of state 3/state 4 in HFD+STZ group is reduced as compared to NCD. There is a rise in the OCR in the P+LG treated group, and **C) Complex III:** OCR of state 3/state 4 in HFD+STZ group is reduced as compared to NCD. There is a rise in the OCR in the P+LG treated group. ($^{@}p$<0.05, $^{@@}p$<0.01, $^{@@@}p$<0.001, vs. HFD+STZ, **p<0.01, ***p<0.001, vs. NCD, n=3/group)

3.3.6 Western blot analysis

The levels of key insulin signalling pathway molecules were estimated by western blot. There was significant decrease in the IR1β, pAkt/tAkt and AdipoR1 expression levels in the HFD+STZ group (p<0.01, p<0.05 and p<0.01, respectively; Figure 3.10 B, C & E). The protein levels were restored in the combination treated group for IR1β, pAkt/tAkt, and AdipoR1 (p<0.001, p<0.01, and p<0.01, respectively; Figure 3.10 B, C & E). Further, there was a significant increase in the IR1β levels in P, LG groups as compared to HFD+STZ (p<0.05 and p<0.01, respectively; Figure 3.10 B). However, no significant difference was observed in the PPARα levels (ns=non-significant; Fig 3.10 F).

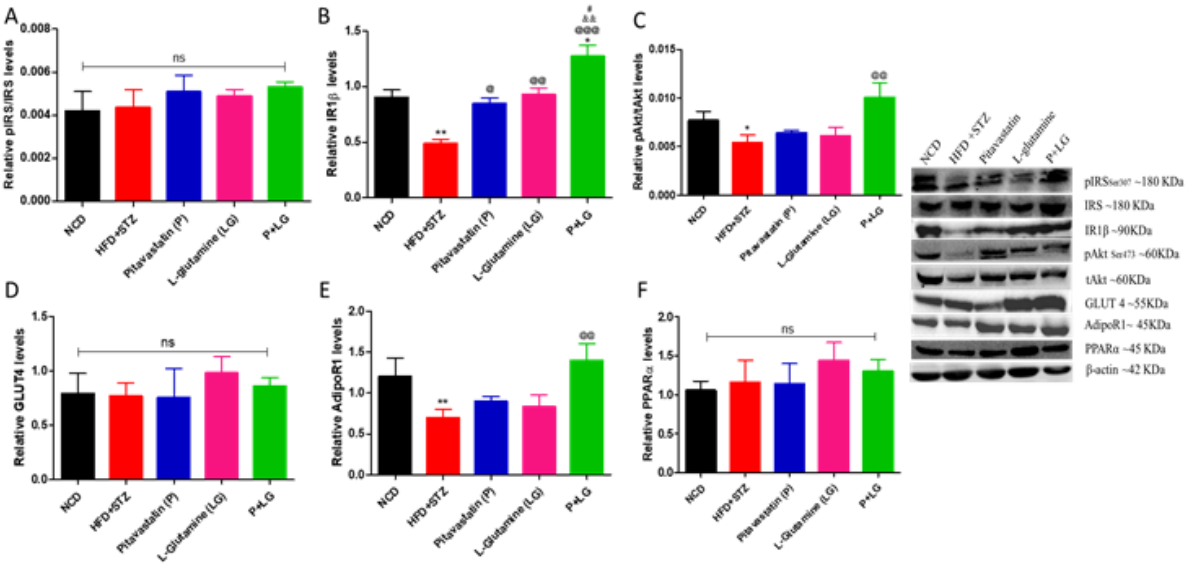

Figure 3.10. Insulin signalling pathway: A) pIRS/IRS ratio: There was no significant difference in the pIRS/IRS ratio amongst the various groups; **B) Insulin receptor1β:** There was significant decrease in the expression of IR1β in the HFD+STZ group as compared to NCD. A significant increase in the expression of IR1β in the combination treated group as compared to HFD+STZ group and individual treated groups was observed; **C) pAkt/tAkt ratio:** There was a significant decrease in the pAkt/tAkt ratio in the HFD+STZ group as compared to NCD. A significant rise in the pAkt/tAkt ratio was observed in the combination treated group as compared to HFD+STZ**; D) GLUT4:** There was no significant difference in the GLUT4 levels amongst the various groups; **E) AdipoR1:** There was a significant decrease in the AdipoR1 expression in the HFD+STZ group as compared to NCD. A significant rise in the AdipoR1 levels was observed in the combination treated group as

compared to HFD+STZ group; **E) PPARα:** There was no significant difference in the PPARα levels amongst the various groups. ($^{@@}p$<0.01, $^{@@@}p$<0.001, vs. HFD+STZ, $^{\&\&}p$<0.01, vs. P, $^{\#}p$<0.05, vs. LG, $^{*}p$<0.05, $^{**}p$<0.01, vs. NCD, n=3/group).

3.3.7 Regeneration and apoptosis analysis in pancreatic β-cells:

A significant destruction of insulin positive β-cells was seen in the HFD+STZ group with a significant increase in the number of apoptotic β-cells (p<0.001; Figure 3.11 A, B, C, D & E) and reduced number of islets/pancreatic section (p<0.01; Figure 3.11 F) as compared to NCD. Upon treatment there was a significant rise in the insulin/BrdU co-positive cells in P, LG and P+LG groups as compared to HFD+STZ (p<0.05, p<0.05 and p<0.001, respectively; Figure 3.11 A and A'). Further, markers for neogenesis (Pdx1 and Ngn3), and transdifferentiation (Pax4 and Arx) were co-stained with insulin and it was observed that only Pdx1 and Pax4 were co-stained with insulin (p<0.05, p<0.05 and p<0.01, and p<0.05, p<0.51 and p<0.001, respectively; Figure 3.11 B & B', and C & C', respectively) upon mono- and combination treatment. No Ngn3 and Arx1 positive cells were found. There was a significant increase in the insulin/TUNEL positive cells in the HFD+STZ group (p<0.001) which was reversed upon the treatment with mono- and combination therapies (p<0.001, p<0.001 & p<0.001, respectively; Figure 3.11 D and D'). Further, a significant decrease in the number of islets) was observed in the HFD+STZ group (p<0.01; Figure 3.11 F). However, no AIF translocation was observed in the HFD+STZ group (Figure 3.11 E). Overall, there was a significant increase in the number of Islets/pancreatic section in the combination treated groups as compared to HFD+STZ group (p<0.001; Figure 3.11 F).

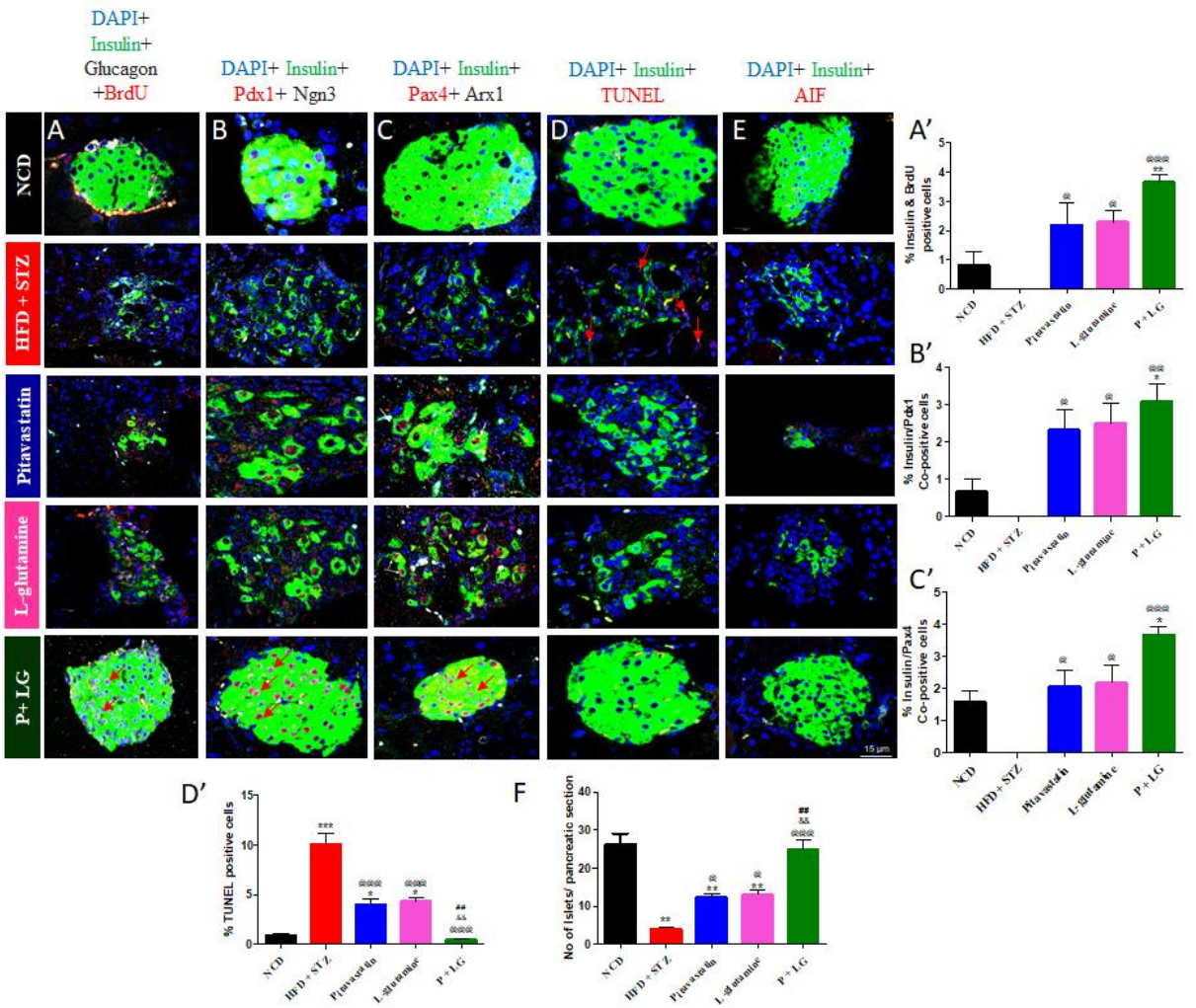

Figure 3.11. Immuno-histochemistry of pancreatic Islets of Langerhans at 60X: A & A') Proliferation: BrdU positive cells were not observed in HFD+STZ group. A significant increase in the Insulin/BrdU co-positive cells was observed in P, LG and P+LG treated groups as compared to HFD+STZ; **B & B') Neogenesis (Insulin/Pdx1/Ngn3):** Pdx1/Ngn3 positive cells were not observed in HFD+STZ group. Upon treatment a significant increase in only Insulin/Pdx1 co-positive cells was observed in the P, LG and P+LG groups as compared to HFD+STZ; **C & C') Transdifferentiation (Insulin/Pax4/Arx1):** No Pax4/Arx1 positive cells were observed in the HFD+STZ group while a significant increase was observed in the P, LG and P+LG groups as compared to HFD+STZ; **D & D') TUNEL:** A significant increase in the insulin/TUNEL positive cells was observed in the HFD+STZ group which decreased significantly in the P, LG and P+LG groups; **E) AIF:** No significant translocation of AIF was observed in any of the groups. **F) Number of Islets/pancreatic section:** A significant decrease in the number of Islets/pancreatic section was observed in the HFD+STZ group.

Also, there were a few insulin-positive cells HFD+STZ group. A significant increase in number of Islets/pancreatic section was observed in P, LG and P+LG groups as compared to HFD+STZ ($^{@}p<0.05$, $^{@@}p<0.01$, $^{@@@}p<0.001$, vs. HFD+STZ, $^{\&\&}p<0.01$, vs. P, $^{\#\#}p<0.01$, vs. LG, $*p<0.05$, $**p<0.01$, $***p<0.001$, vs. NCD, n=3/group, Scale= 20µm, Magnification= 60X).

3.4. Discussion

Our results demonstrate that pitavastatin and L-glutamine in combination could ameliorate T2D manifestations by 1) improving glucose tolerance and insulin sensitivity, 2) normalizing insulin and adiponectin levels, 3) inhibiting gluconeogenesis, reducing hepatic GLUT2 and enhancing glycolysis, glycogen synthesis, 4) increasing IR1β, pAKT, and AdipoR1 expression levels in skeletal muscle, 5) increasing mitochondrial biogenesis and ETC activities, and 6) increasing β-cell regeneration by proliferation (Fig 3.12).

Obesity is strongly associated with a reduction in anti-inflammatory and increase in pro-inflammatory adipokines. Many of these adipokines are crucial in maintaining insulin sensitivity of peripheral tissues viz. adipose tissue and skeletal muscle (Pramanik *et al*., 2017; Patel *et al*., 2016; Patel *et al*.; 2018; Patel *et al*.; 2019; Rathwa *et al*., 2019 a & b; Rathwa *et al*., 2020). Due to this, regulating hyperglycemia by regulating only the hepatic glucose output or enhancing glucose clearance seems superficial. Also, T2D patients show a significant reduction in β-cell mass. Thus, to ameliorate glucolipotoxicity and β-cell loss, we selected pitavastatin and L-glutamine, as pitavastatin lowers blood and tissue cholesterol levels, while enhancing adiponectin, and L-glutamine exhibits incretin secretagogue property. We found that in hyperlipidemic T2D conditions, pitavastatin was effective in bringing about glucose homeostasis, increasing adiponectin levels and reducing TC, TG and LDL. Previous studies also reported the ability of statins to enhance glucose tolerance and increase anti-inflammatory adipokines by lowering LDL and c-reactive proteins (Lee *et al*., 2016; Yoshika *et al*., 2010; Matsubara *et al*., 2012; Iwata *et al*., 2019; Chen *et al*., 2019; Cho *et al*., 2020). *In vitro* studies suggest that the off-target effect of pitavastatin on adiponectin may be related to the prevention of adipocyte hypertrophy and adipokine dysregulation (Ishihara *et al*., 2010). The L-Glutamine treated group also showed enhanced glucose homeostasis (Greenfield *et al*., 2009; Molfino *et al*., 2009; Samocha-Bonet *et al*., 2011), increased adiponectin levels (Abboud *et al*., 2019) and reduced TG, TC and LDL levels (Alba-Loureiro *et al*., 2009;

Badole *et al*., 2013). As reported earlier, we also found increased insulin in the L- Glutamine treated group (Abboud *et al*., 2019; Badole *et al*., 2013). In liver it is converted to L-alanine which is consumed at a high rate by β-cells exerting an insulinotropic effect (Newsholme *et al*., 2006). Interestingly, while the two drugs could individually show dramatic increase in the adiponectin levels, the combination could only bring about normoadiponectinemia. We hypothesized the dramatic increase in adiponectin levels would be for not being able to activate the adiponectin signalling pathway, and we found the protein expression of AdipoR1 was not significant in the monotherapies as compared to HFD+STZ group, while its expression was significantly increased in the combination group. AdipoR1 deficiency impairs adiponectin-induced AMP-activated protein kinase (AMPK) activation resulting in impaired glucose transport, mitochondrial biogenesis and fatty acid oxidation (Kim and Park, 2016; Sun *et al*., 2017). However, we did not see a significant change in the levels of PPARα, a downstream transcription factor activated upon adiponectin binding to AdipoR1 suggesting its dominant crosstalk with the insulin signalling pathway to bring about glucose homeostasis in the combination treatment (Ruan and Dong, 2016). However, the combination treatment enhanced insulin levels, glucose tolerance, insulin sensitivity, FBG levels, and improved lipid profile as a consequence of increased adiponectin signalling pathway. Further, adiponectin is well known to suppress hepatic glucose output and lower systemic glucose by enhancing hepatic insulin sensitivity, and inhibiting expression and activity of gluconeogenesis key enzymes (Miller *et al*., 2011; Turer *et al*., 2012). As expected, the glucoregulatory pathway got significantly corrected upon pitavastatin treatment with an increased expression of *GCK* mRNA levels and its activity, increased glycogenesis and glycogen content as supported by Daido *et al*., 2014. We also found decreased insulin resistance and hepatic *GLUT2* mRNA expression. Supporting our results Fraulob *et al*. also reported amelioration of insulin resistance, and hepatic steatosis in HFD fed C57BL/6J mice when treated with rosuvastatin (Fraulob *et al*., 2012). Thus, contradictory to reports stating statins cause new onset diabetes, we propose that statins do not lead to glucose overproduction in an already hyperlipidemic state of T2D. In addition, we also found a concomitant decrease in the *PEPCK* and *FBPase* transcript levels and activities. The cleaved GLP-1 product suppresses gluconeogenesis and also acts as an antioxidant (Thomas and Habener, 2010) and predictably L-glutamine was also found to enhance the glucoregulatory pathway by reducing hepatic glucose output, increasing glycogen synthesis and decreasing *GLUT2* expression as a result of reduced

glycogen phosphorylase expression. Overall, P+LG combination could enhance the hepatic glucoregulatory pathway by inhibiting gluconeogenesis, reducing *GLUT2* expression, and increasing glycolysis resulting in normoglycemia. We also report significantly enhanced insulin signalling pathway leading to glucose uptake in mono- and combination therapies. This is the first report wherein the effect of pitavastatin on insulin signalling pathway was studied *in-vivo*. APPL1 (down-stream effector of AdipoR1) interacts with IR1β driving the insulin signalling cascade forward, resulting in phosphorylation of Akt (Ryu *et al.,* 2014). However, we did not find any change in the GLUT4 expression as we measured the total GLUT4. Nonetheless, the increased insulin sensitivity and glucose tolerance suggests an ultimate rise in the membrane translocated GLUT4.

Glucolipotoxicity is known to induce oxidative stress and mitochondrial dysfunction. Further, pitavastatin could increase the transcript levels of *PGC1α, TFAM* and *SIRT1*, thus alleviating oxidative stress, and enhance the electron transport chain (ETC) complexes I and III activities as reinforced by previous studies (Ota *et al*., 2010, Vevera *et al*., 2016). Our results for the first time suggest that L-glutamine being an antioxidant, maintains mitochondrial integrity by inducing mitochondrial biogenesis, and increasing complex I and III activities. Thus, here too we saw a combinatorial effect of the drugs on mitochondrial biogenesis and ETC complexes I, II & III activities. Finally, our immunohistochemistry data suggests significant reduction in β-cell death in both mono- and combination therapies. Further, pitavastatin and L-glutamine could induce β-cell proliferation as the insulin positive β-cells expressed Pdx1 and Pax4 along with a significant incorporation of BrdU in the nucleus. Zhao and Zhao found that β-cells treated with low dose of pitavastatin were in S and G_2/M phase as compared to other statin groups *in-vitro* (Zhao and Zhao, 2015). Moullé *et al*., found that L-glutamine controlled the biosynthesis of IGF2, an autocrine regulator of β-cell mass and function and activates Akt phosphorylation in β-cells leading to its proliferation (Moullé *et al*., 2017). L-glutamine has also been reported to be able to upregulate Pdx1 (Corless *et al*., 2006). Pdx1in concert with Ngn3 and Mafa is an important marker of islet neogenesis (differentiation of acinar cells to β-cells), while Pax4 is a marker of transdifferentiation (α- to β-cell conversion) (Zhu *et al*., 2015; Zhang *et al*., 2016). However, we did not find Ngn3 and insulin co-positive cells. Hence, our data indicates significant increase in β-cells via proliferative pathway alone. Though there was only a marginally significant increase in the number of islets in

monotherapies, they showed an increase in Pdx1 and Pax4 insulin co-positive cells demonstrating their individual β-cell regenerative properties. Pax4 was also reported to promote differentiation of Pdx1 positive mesenchymal stem cells to β-cell fate (Xu *et al*., 2017). Future studies in this direction are warranted.

Three large meta-analyses of randomized, controlled trials showed those who are >60 years of age or who are undergoing an intensive-dose of statin therapy have higher chances of developing new onset diabetes (Rajpathak *et al*., 2009; Sattar *et al*., 2010; Preiss *et al*., 2011), but our results clearly state that effect of statin is largely based on the dosage recommended. Combination therapy has been proven to have several advantages compared to stepwise treatment modules, including a multidirectional approach to the problem and this has been substantiated in other unpublished studies by our group (Rathwa *et al*., 2021; Roma *et al*., 2019). We hypothesize that, pitavastatin's and L-glutamine's individual adiponectin enhancing properties, coupled with their combinatorial AdipoR1 expression enhancing property resulted in the significant correction of T2D manifestations. Though several preclinical and clinical studies have been carried out to explore the individual therapeutic potential of pitavastatin and L-glutamine to ameliorate T2D, this is the first study to explore the combination effect of the two drugs on various diabetes manifestations.

A point worth mentioning here is that combination of dipeptidyl peptidase 4 (DPP4) inhibitor sitagliptin (extends GLP-1 half-life) in combination with simvastatin was approved by the US Food and Drug Administration in October 2011 and sold under the brand name Juvisync. It is a fixed-dose combination of anti-diabetic medication used to treat T2D and hypercholesterolemia (Ramadan *et al*., 2015).

Future studies are needed to understand the mechanism of adiponectin potentiating action, increasing AdipoR1 expression and β-cell proliferation of the combination therapy.

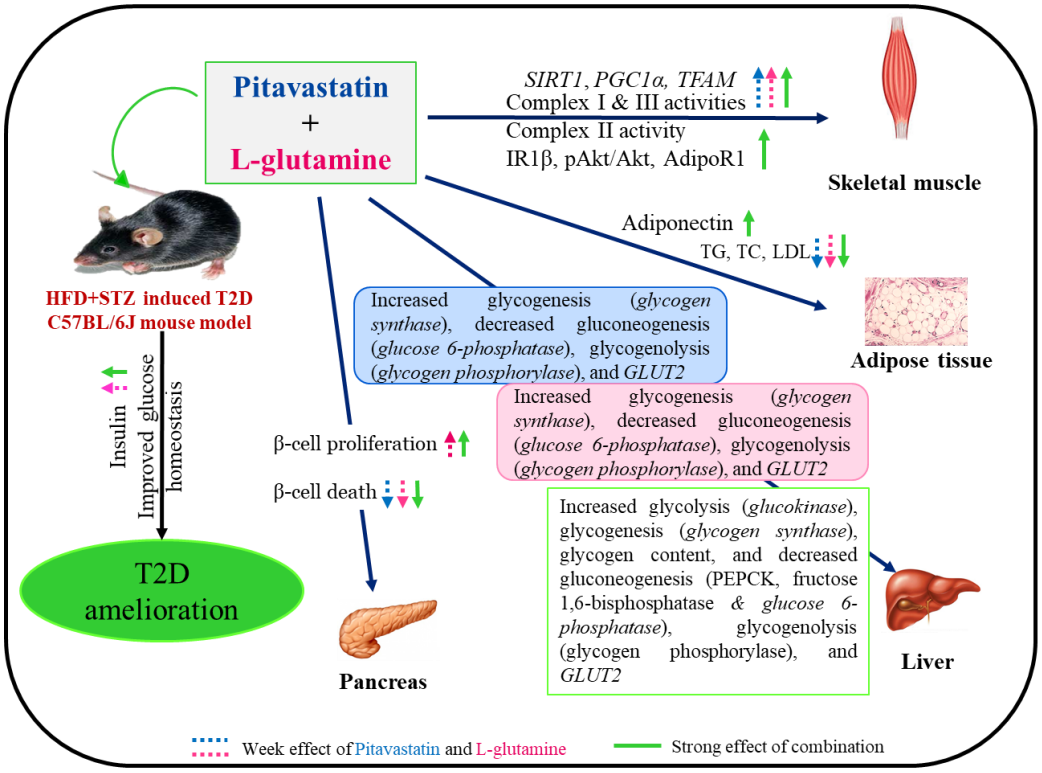

Figure 3.12: Effect of pitavastatin, L-glutamine and the combination therapy on amelioration of T2D manifestations: Pitavastatin and L-glutamine could induce normolipidemia and reduce the transcript levels of *glucose 6-phosphatase, glycogen phosphorylase* and *GLUT2* in liver whilst increasing *SIRT1, PGC1α* and *TFAM*, mitochondrial ETC complexes I and III activities in skeletal muscle. Both pitavastatin and L-glutamine could also reduce β-cell death individually and L-glutamine also could induce β-cell proliferation. In combination they could additionally increase mitochondrial ETC complex III activity in skeletal muscle, and *glucokinase* transcript levels with a concomitant decrease in PEPCK and fructose 1,6-bisphophatase activities in liver. The combination therapy also induced normoadiponectinemia, increased pAkt/Akt, increased IR1β and AdipoR1 protein levels in skeletal muscle, and increased plasma insulin levels. Thus, the drugs together could bring about normolipidemia, reverse mitochondrial dysfunction, decrease gluconeogenesis, glycogenolysis, glycogen synthesis and *GLUT2* expression. The combination therapy could also reduce β-cell death, enhance glucose tolerance and insulin sensitivity thus being able to ameliorate T2D in HFD+STZ induced mouse model.

3.5. References:

Abboud, K. Y., Reis, S. K., Martelli, M. E., *et al.* (2019). Oral glutamine supplementation reduces obesity, pro-inflammatory markers, and improves insulin sensitivity in DIO wistar rats and reduces waist circumference in overweight and obese humans. Nutrients, 11(3), 536.

Alba-Loureiro, T. C., Ribeiro, R. F., Zorn, T. M. T., *et al*. (2010). Effects of glutamine supplementation on kidney of diabetic rat. Amino acids, 38(4), 1021-1030.

Badole, S. L., Chaudhari, S. M., Bagul, P. P., *et al.* (2013). Effect of concomitant administration of L-glutamine and cycloart-23-ene-3β, 25-diol (B2) with sitagliptin in GLP-1 (7–36) amide secretion, biochemical and oxidative stress in streptozotocin-nicotinamide induced diabetic sprague dawley rats. PloS one, 8(8), e72817.

Badole, S. L., Jangam, G. B., Chaudhari, S. M., *et al.* (2014). L-glutamine supplementation prevents the development of experimental diabetic cardiomyopathy in streptozotocin-nicotinamide induced diabetic rats. PLoS One, 9(3), e92697.

Bakalar, B., Duska, F., Pachl, J., *et al.* (2006). Parenterally administered dipeptide alanyl-glutamine prevents worsening of insulin sensitivity in multiple-trauma patients. Critical care medicine, 34(2), 381-386.

Bloomgarden, Z. T. (2020). Diabetes and COVID-19. Journal of Diabetes, 12(4), 347-348.

Butler, A. E., Janson, J., Bonner-Weir, S., *et al.* (2003). β-cell deficit and increased β-cell apoptosis in humans with type 2 diabetes. Diabetes, 52(1), 102-110.

Butterick, T. A., Stone, L. H., Duffy, C., *et al.* (2016). Pioglitazone increases PGC1-α signaling within chronically ischemic myocardium. Basic research in cardiology, 111(3), 37.

Cengiz, M., Uysal, B. B., Ikitimur, H., *et al*. (2020). Effect of oral L-Glutamine supplementation on Covid-19 treatment. Clinical nutrition experimental, 33, 24-31.

Chen, L. W., Lin, C. S., *et al.* (2019). Pitavastatin exerts potent anti-inflammatory and immunomodulatory effects via the suppression of AP-1 signal transduction in human T cells. International journal of molecular sciences, 20(14), 3534.

Chen, S., Akter, S., Kuwahara, K., *et al.* (2019). Serum amino acid profiles and risk of type 2 diabetes among Japanese adults in the Hitachi Health Study. Scientific reports, 9(1), 1-9.

Corless, M., Kiely, A., McClenaghan, N. H., *et al.* (2006). Glutamine regulates expression of key transcription factor, signal transduction, metabolic gene, and protein expression in a clonal pancreatic β-cell line. Journal of Endocrinology, *190*(3), 719-727.

Daido, H., Horikawa, Y., & Takeda, J. (2014). The effects of Pitavastatin on glucose metabolism in patients with type 2 diabetes with hypercholesterolemia. Diabetes research and clinical practice, 106(3), 531-537.

Fraulob, J. C., Souza-Mello, V., Aguila, M. B., *et al*. (2012). Beneficial effects of rosuvastatin on insulin resistance, adiposity, inflammatory markers and non-alcoholic fatty liver disease in mice fed on a high-fat diet. Clinical science, 123(4), 259-270.

Garber, A. J. (2011). Incretin effects on β-cell function, replication, and mass: the human perspective. Diabetes care, 34(Supplement 2), S258-S263.

Greenfield, J. R., Farooqi, I. S., Keogh, J. M., *et al.* (2009). Oral glutamine increases circulating glucagon-like peptide 1, glucagon, and insulin concentrations in lean, obese, and type 2 diabetic subjects. The American journal of clinical nutrition, 89(1), 106-113.

Guo, Y., Fu, W., Xin, Y., *et al.* (2018). Antidiabetic and antiobesity effects of artemether in db/db mice. BioMed research international.

Hayek, T., Ito, Y., Azrolan, N., *et al*. (1993). Dietary fat increases high density lipoprotein (HDL) levels both by increasing the transport rates and decreasing the fractional catabolic rates of HDL cholesterol ester and apolipoprotein (Apo) AI. Presentation of a new animal model and mechanistic studies in human Apo AI transgenic and control mice. The Journal of clinical investigation, 91(4), 1665-1671.

Ishihara, Y., Ohmori, K., Mizukawa, M., *et al.* (2010). Beneficial direct adipotropic actions of Pitavastatin in vitro and their manifestations in obese mice. Atherosclerosis, 212(1), 131-138.

Iwata, H., Iimuro, S., Inoue, A., *et al.* (2019). P5320 Reduction in high-sensitivity C-reactive protein by Pitavastatin was associated with improved outcomes in Japanese patients with stable coronary artery disease: results from REAL-CAD study. European Heart Journal, 40(Supplement_1), ehz746-0289.

Jones, C. G., Hare, J. D., & Compton, S. J. (1989). Measuring plant protein with the Bradford assay. Journal of chemical ecology, 15(3), 979-992.

Jørgensen, M. S., Tornqvist, K. S., & Hvid, H. (2017). Calculation of glucose dose for intraperitoneal glucose tolerance tests in lean and obese mice. Journal of the American Association for Laboratory Animal Science, 56(1), 95-97.

Kim, D. W., Kim, D. H., Park, J. H., *et al.* (2019). Association between statin treatment and new-onset diabetes mellitus: a population based case–control study. Diabetology & metabolic syndrome, 11(1), 30.

Kim, Y., & Park, C. W. (2016). Adenosine monophosphate–activated protein kinase in diabetic nephropathy. Kidney research and clinical practice, 35(2), 69-77.

Knopfholz, J., Disserol, C. C. D., Pierin, A. J., *et al.* (2014). Validation of the friedewald formula in patients with metabolic syndrome. Cholesterol.

Lee, S., Lee, Y., Kim, J., *et al.* (2016). Atorvastatin and rosuvastatin improve physiological parameters and alleviate immune dysfunction in metabolic disorders. Biochemical and biophysical research communications, 478(3), 1242-1247.

Li, Z., & Graham, B. H. (2012). Measurement of mitochondrial oxygen consumption using a Clark electrode. In Mitochondrial Disorders (pp. 63-72). Humana Press.

Matsubara, T., Naruse, K., Arakawa, T., *et al.* (2012). Impact of Pitavastatin on high-sensitivity C-reactive protein and adiponectin in hypercholesterolemic patients with the metabolic syndrome: the PREMIUM Study. Journal of cardiology, 60(5), 389-394.

Matveyenko, A. V., & Butler, P. C. (2008). Relationship between β-cell mass and diabetes onset. Diabetes, Obesity and Metabolism, 10, 23-31.

Miller, R. A., Chu, Q., Le Lay, J., *et al.* (2011). Adiponectin suppresses gluconeogenic gene expression in mouse hepatocytes independent of LKB1-AMPK signaling. The Journal of clinical investigation, 121(6), 2518-2528.

Mita, T., Nakayama, S., Abe, H., *et al*. (2013). Comparison of effects of Pitavastatin and atorvastatin on glucose metabolism in type 2 diabetic patients with hypercholesterolemia. Journal of diabetes investigation, 4(3), 297-303.

Molfino, A., Logorelli, F., Muscaritoli, M., *et al.* (2010). Metabolic effects of glutamine on insulin sensitivity. Nutritional Therapy & Metabolism, 28(1).

Moullé, V. S., Ghislain, J., & Poitout, V. (2017). Nutrient regulation of pancreatic β-cell proliferation. Biochimie, 143, 10-17.

Newsholme, P., Brennan, L., & Bender, K. (2006). Amino acid metabolism, β-cell function, and diabetes. Diabetes, 55(Supplement 2), S39-S47.

Ota, H., Eto, M., Kano, M. R., *et al.* (2010). Induction of endothelial nitric oxide synthase, SIRT1, and catalase by statins inhibits endothelial senescence through the Akt pathway. Arteriosclerosis, thrombosis, and vascular biology, 30(11), 2205-2211.

Owei, I., Umekwe, N., Stentz, F., *et al.* (2019). Amino acid signature predictive of incident prediabetes: A case-control study nested within the longitudinal pathobiology of prediabetes in a biracial cohort. Metabolism, 98, 76-83.

Palit, S. P., Patel, R., Jadeja, S. D., *et al.* (2020). A genetic analysis identifies a haplotype at adiponectin locus: association with obesity and type 2 diabetes. Scientific reports, 10(1), 1-10.

Parilla, J. H., Willard, J. R., Barrow, B. M., & Zraika, S. (2018). A mouse model of beta-cell dysfunction as seen in human type 2 diabetes. Journal of diabetes research.

Patel, R., Dwivedi, M., Mansuri, M. S., *et al.* (2016). Association of neuropeptide-Y (NPY) and interleukin-1beta (IL1B), genotype-phenotype correlation and plasma lipids with Type-II diabetes. PloS one, 11(10), e0164437.

Patel, R., Palit, S. P., Rathwa, N., *et al.* (2019). Genetic variants of tumor necrosis factor-α and its levels: A correlation with dyslipidemia and type 2 diabetes susceptibility. Clinical nutrition, 38(3), 1414-1422.

Patel, R., Pramanik, S., Rathwa, N. N., *et al.* (2019). 112-LB: Melatonin and DPP-IV Inhibitor: A Novel Combinatorial Approach for ß-Cell Regeneration. DOI: https://doi.org/10.2337/db19-112-LB

Patel, R., Rathwa, N., Palit, S. P., *et al.* (2018). Association of melatonin & MTNR1B variants with type 2 diabetes in Gujarat population. Biomedicine & Pharmacotherapy, 103, 429-434.

Pramanik, S., Rathwa, N., Patel, R., *et al.* (2018). Treatment avenues for type 2 diabetes and current perspectives on adipokines. Current diabetes reviews, 14(3), 201-221.

Preiss, D., Seshasai, S. R. K., Welsh, P., *et al.* (2011). Risk of incident diabetes with intensive-dose compared with moderate-dose statin therapy: a meta-analysis. Jama, 305(24), 2556-2564.

Rajpathak, S. N., Kumbhani, D. J., Crandall, J., *et al.* (2009). Statin therapy and risk of developing type 2 diabetes: a meta-analysis. Diabetes care, 32(10), 1924-1929.

Rathwa, N., Parmar, N., Palit, S. P., *et al.* (2020). Intron specific polymorphic site of vaspin gene along with vaspin circulatory levels can influence pathophysiology of type 2 diabetes. Life sciences, 243, 117285.

Rathwa, N., Parmar, N., Palit, S. P., *et al.* (2021). Calorie Restriction in combination with GABA: improved glycaemic control in type 2 diabetes mouse model. bioRxiv doi: https://doi.org/10.1101/2021.05.12.443226.

Rathwa, N., Patel, R., Palit, S. P., *et al.* (2019a). Circulatory Omentin-1 levels but not genetic variants influence the pathophysiology of Type 2 diabetes. Cytokine, 119, 144-151.

Rathwa, N., Patel, R., Palit, S. P., *et al.* (2019b). Genetic variants of resistin and its plasma levels: Association with obesity and dyslipidemia related to type 2 diabetes susceptibility. Genomics, 111(4), 980-985.

Ruan, H., & Dong, L. Q. (2016). Adiponectin signaling and function in insulin target tissues. Journal of molecular cell biology, 8(2), 101-109.

Ryu, J., Galan, A. K., Xin, X., *et al*. (2014). APPL1 potentiates insulin sensitivity by facilitating the binding of IRS1/2 to the insulin receptor. Cell reports, 7(4), 1227-1238.

Sadar, S., Kaspate, D., & Vyawahare, N. (2016). Protective effect of L-glutamine against diabetes-induced nephropathy in experimental animal: role of KIM-1, NGAL, TGF-β1, and collagen-1. Renal failure, 38(9), 1483-1495.

Samocha-Bonet, D., Wong, O., Synnott, E. L., *et al.* (2011). Glutamine reduces postprandial glycemia and augments the glucagon-like peptide-1 response in type 2 diabetes patients. The Journal of nutrition, 141(7), 1233-1238.

Sattar, N., Preiss, D., Murray, H. M., *et al.* (2010). Statins and risk of incident diabetes: a collaborative meta-analysis of randomised statin trials. The Lancet, 375(9716), 735-742.

Stoscheck, C. M. (1990). [6] Quantitation of protein. Methods in enzymology, 182, 50-68.

Sun, L., Yang, X., Li, Q., *et al.* (2017). Activation of adiponectin receptor regulates proprotein convertase subtilisin/kexin type 9 expression and inhibits lesions in ApoE-deficient mice. Arteriosclerosis, thrombosis, and vascular biology, 37(7), 1290-1300.

Tomas, E., & Habener, J. F. (2010). Insulin-like actions of glucagon-like peptide-1: a dual receptor hypothesis. Trends in Endocrinology & Metabolism, 21(2), 59-67.

Tolhurst, G., Zheng, Y., Parker, H. E., *et al.* (2011). Glutamine triggers and potentiates glucagon-like peptide-1 secretion by raising cytosolic Ca2+ and cAMP. Endocrinology, 152(2), 405-413.

Tsai, P. H., Liu, J. J., Yeh, C. L., *et al.* (2012). Effects of glutamine supplementation on oxidative stress-related gene expression and antioxidant properties in rats with streptozotocin-induced type 2 diabetes. British journal of nutrition, 107(8), 1112-1118.

Turer, A. T., & Scherer, P. E. (2012). Adiponectin: mechanistic insights and clinical implications. Diabetologia, 55(9), 2319-2326.

Varnier, M. A. U. R. I. Z. I. O., Leese, G. P., Thompson, J. A. M. E. S., *et al*. (1995). Stimulatory effect of glutamine on glycogen accumulation in human skeletal muscle. American Journal of Physiology-Endocrinology and Metabolism, 269(2), E309-E315.

Vevera, J., Fisar, Z., Nekovarova, T., *et al* (2016). Statin-induced changes in mitochondrial respiration in blood platelets in rats and human with dyslipidemia. Physiological research, 65(5), 777.

Xu, L., Xu, C., Zhou, S., *et al.* (2017). PAX4 promotes PDX1-induced differentiation of mesenchymal stem cells into insulin-secreting cells. American journal of translational research, 9(3), 874.

Yoshika, M., Komiyama, Y., Masuda, M., *et al.* (2010). Pitavastatin further decreases serum high-sensitive C-reactive protein levels in hypertensive patients with hypercholesterolemia treated with angiotensin II, type-1 receptor antagonists. Clinical and Experimental Hypertension, 32(6), 341-346.

Zambarakji, H. J., Nakazawa, T., Connolly, E., *et al.* (2006). Dose-dependent effect of Pitavastatin on VEGF and angiogenesis in a mouse model of choroidal neovascularization. Investigative ophthalmology & visual science, 47(6), 2623-2631.

Zhang, Y., Fava, G. E., Wang, H., *et al.* (2016). PAX4 gene transfer induces α-to-β-cell phenotypic conversion and confers therapeutic benefits for diabetes treatment. Molecular Therapy, 24(2), 251-260.

Zhao, W., & Zhao, S. P. (2015). Different effects of statins on induction of diabetes mellitus: an experimental study. Drug design, development and therapy, 9, 6211.

Zhu, Y., Liu, Q., Zhou, Z., *et al.* (2017). PDX1, Neurogenin-3, and MAFA: critical transcription regulators for β-cell development and regeneration. Stem cell research & therapy, 8(1), 1-7.